Central Asian Journal of Environmental Science and Technology Innovation **6** (2020) 310–329

RESEARCH PAPER

Kinetic and equilibrium studies of adsorptive removal of sodium-ion onto wheat straw and rice husk wastes

Akbar Rasouli [1], Ali Bafkar [2*], Zeinab Chaghakaboodi [3]

[1] Department of Irrigation and Drainage Engineering, Razi University, Kermanshah, Iran

[2] Department of Water Engineering, Razi University, Kermanshah, Iran

[3] Department of Production Engineering and Plant Genetics, Faculty of Science and Agricultural Engineering, Razi University, Kermanshah, Iran

Highlights

- The existence of chemical solutes in water and soil resources is main environmental problems.
- The removal of sodium onto the wheat straw and rice husk wastes nanostructured sorbents has been evaluated.
- The increasing in pH from 3 to 5 and contact time caused increased adsorption efficiency.
- The adsorption capacity increased in the wheat straw and rice husk wastes sorbents from 0.34 to 9.43 mg and 0.36 to 9.43 mg, respectively.

Graphical Abstract

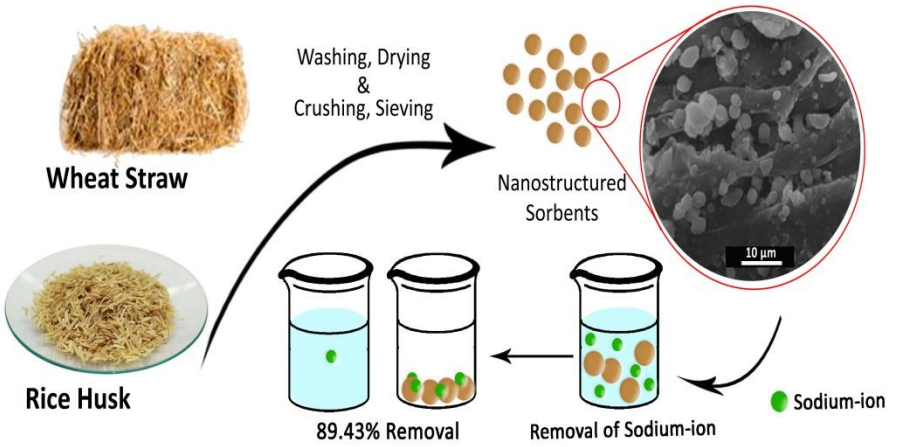

Article Info

Receive Date: 15 November 2020
Revise Date: 05 December 2020
Accept Date: 20 December 2020
Available online: 25 December 2020

Keywords:
Adsorption
Kinetic
Isotherm
Sodium
Wheat straw
Rice husk wastes

Abstract

The presence of solutes in water and soil resources is one of the main environmental problems of many societies. The purpose of this study was to evaluate and compare the removal of sodium onto the wheat straw and rice husk wastes nanostructured sorbents. This study was conducted in a batch experiment scale with changes in effective factors such as pH (4.3, 5, 6, 7, and 8), contact time (10, 30, 60, 90, 120, and 180 minutes), sorbent dosage (0.3, 0.5, 0.7, 1, 1.3, and 1.6 g), and the initial concentration (5, 10, 30, 60, 90, and 120 mg/L) of sodium metal solution were investigated. Sodium adsorption kinetics on the prepared sorbent was examined based on isotherms of absorption equations. The results showed that the adsorption efficiency of the sorbent studied increases the increasing in pH from 3 to 5, but that the metal ion deposited at a pH greater than 5. Increasing the contact time increases the adsorptive efficiency. In addition, efficiency first increased and then, decreased by increasing the amount of nanometer sorbent. Increasing the initial concentration of sodium from 5 to 120 mg/L for the wheat straw and rice husk wastes sorbents cause decreasing the adsorption efficiency from 85.49 to 68.07% and 89.43 to 68.2% due to lack of sufficient adsorbent higher sodium ion content. Consequently, the adsorption capacity increased from 0.34 to 9.43 mg and 0.36 to 9.43 mg.

10.22034/CAJESTI.2020.06.04

E-ISSN: 2717-0519
P-ISSN: 2717-4034

*Corresponding author: alibafkar@yahoo.com (A. Bafkar)

1. Introduction

Water scarcity threatens more than 88 developing countries, which include more than half of the world's population. About 80 to 90% of the diseases and 30% of deaths in these countries are due to poor water quality. Over the next 25 years, the number of people facing water scarcity will increase four times. Therefore, the low-cost desalination methods of saline water and seawater will be considered. Over the past 60 years, much attention has been devoted to desalination. Desalination is a technical tool for increasing freshwater resources, whether in areas with limited water resources or areas with saline and brackish water sources such as underground saline water, drainage water, and saline wastewater. According to available statistics, around 7,500 million cubic meters (MCM) of saline water is desalinized, which is about 0.2% of the world's total water use. The exploration of freshwater from seawater has been studied by many Mediterranean and Middle Eastern countries, but the growth of modern desalination began in 1960 by some Persian Gulf basin countries. Extensive research has also begun to commercialize desalination practices in the United States since 1960. Sodium is one of the mineral chemicals, which are usually found naturally and a certain level of which is necessary for the human body. The exceeded amount of sodium is harmful to human health. One of the most important effects is hypertension (Chaghakaboodi et al., 2021; Zeidali et al., 2021b; Haghshenas and Ghanbari, 2021; Farokhian et al., 2021).

The Institute of Standards and Industrial Research of Iran also announced the maximum allowed amount of sodium in drinking water as much as 200 mg/L and up to 250 mg/L is allowed in the absence of a high-quality water resource in the region. There are various methods for removing metals from water and sewage. The disadvantages of these methods are pre-purification for removing suspended materials, high cost, and being time-consuming (Juang et al., 2003; Liang et al., 2020). One of the fundamental solutions to overcome the deficiencies of conventional purification methods is the use of nanotechnology. Nanotechnology is a process that plays a key role in preventing pollution, detecting, measuring, and purifying the pollutants. Nanoparticles, due to their small size, high cross-sectional area, crystalline shape and unique network order, can be used to filter, and convert pollutants into harmless and less harmful substances because of high reactivity (Samadi et al., 2010). The smaller size of the particles of the sorbent material with nearly more spherical shape causes more contact with the fluid phase, which increases the speed of the adsorption process (Gupta et al., 2003). Over the past years, a large number of industrial and agricultural waste have been successfully used by various researchers as potential absorbers for the removal of various pollutants from water and sewage (Kahrizi et al., 2016).

Sfaksi et al., 2014 examined the removal of six volumes of chromium from water by cork waste (Sfaksi et al., 2014). The results showed that the removal percentage depends on the contact time, particle size, temperature, initial concentration of chromium, and pH of the system, and pH had the highest effect among all the parameters. The maximum adsorption of chromium occurred at pH in the range of 2.5-3. El-Sadaawy and Abdelwahab, 2014 examined the removal of nickel from aqueous solutions using the activated carbon obtained from the African palm kernel shells (El-Sadaawy and Abdelwahab, 2014). The results showed that maximum nickel adsorption for raw materials, type 1 carbon, and carbon type 2 at PH=7 was as much as 40.68, 49.15, and 50.68%, respectively. Tounsadi et al., 2015 investigated the removal of cadmium and cobalt from aqueous solution by Diplotaxis and Chrysanthemums (Tounsadi et al., 2015). The effects of factors such as pH, equilibrium time, sorbent dosage, initial concentration of metal ions, and temperature were evaluated in batch experiments. Also, the effect of sodium, potassium, magnesium, calcium, and aluminium ions was considered on the adsorption process. The results showed that the maximum adsorption efficiency was at pH as much as 6.5 and 7.5. Kinetic studies showed that the Kinetic model of Hou et al., was the best model for describing the adsorption of heavy metals on the adsorbent (Hou et al., 2018). Among isotherm models, the Freundlich model had the highest correlation with experimental data. They also stated that temperature has no significant effect on the adsorption process. Matouq et al., 2015 investigated the removal of copper, nickel, chromium, and zinc metals by a kind of *Moringa oleifera* (Drumstick tree) (Matouq et al., 2015). The effects of factors such as the

initial concentration of metals, contact time, temperature, and sorbent dosage have been evaluated. In order to study the adsorption process Langmuir, Freundlich, Temkin, and Dobbin isotherms models were applied. According to the results, the Freundlich, and Temkin isotherm model were the most correlated with the experimental data for copper and the Temkin and Dobbin isotherms models were introduced as the best model for Chromium. The adsorption capacity for copper, nickel, and chromium ions was as much as 6.07, 5.53, and 5.497 mg/g, respectively.

In addition, the adsorption efficiency for the mentioned metals was 90, 68, and 91%, respectively. Kinetic studies also showed that the Kinetic model of Ho et al., 2018 had the best correlation for all metals (Hou et al., 2018). Singha and Das, 2013 evaluated the removal of copper from aqueous solution by natural agricultural biomass (Singha and Das, 2013). They also investigated the effect of the physicochemical parameters of pH, the initial concentration of the copper ion, contact time, sorbent dosage, and temperature. The results showed that the optimum pH value was as much as 6. The Kinetic model of Ho et al., was the best model to describe the adsorption process by the sorbent and Freundlich and Halsey Isotherm models had the highest consistency with experimental data (Hou et al., 2018). Montanher et al., 2005 concluded that rice bran has high efficiency in removing heavy metals such as divalent cadmium, copper, lead, and zinc from wastewater (Montanher et al., 2005). The results of research carried out by Asrari et al., 2010 indicate that rice bran is a suitable sorbent for heavy metals such as lead and zinc (Asrari et al., 2010). In this regard, the adsorption rate is significantly correlated with pH, sorbent dosage, and contact time parameters. Gao et al., 2008 reported that rice bran as a low-cost sorbent material could be used to remove the Hexavalent chromium [Cr (VI)] metal from wastewater with a high-efficiency (Gao et al., 2008). Also, was investigated the removal of lead metal from sewage using tea waste as a cheap sorbent. The optimal pH was in the range of 5 to 6, and 96.4% of it was eliminated. Also, the waste of coffee in the same condition eliminated 10.5% of the lead. Experiments were carried out in 60 minutes in a batch experiment (Bakhshi et al., 2021; Zeidali et al., 2021a).

Rice, cultivated in more than 75 countries around the world, is considered as the main food for half the world's population. Around 80 million tons of rice husks is produced annually and about 97% of its production comes from developing countries (Armesto et al., 2002). Wheat straw and rice husk wastes make the adsorption process desirable due to its rich strands, protein, silica, and specific functional groups (Han et al., 2006). Therefore, the present research aimed to evaluate the efficiency of wheat straw and rice husk Nano-structure sorbents as waste material with features such as grain structure and water solubility in water, chemical stability, and local access for the removal of sodium element from laboratory wastewater (Zulkali et al., 2006).

2. Material and Methods

This study has employed an experimental-applied research method in the form of batch experiments (Discontinuous). Metal solutions with a volume of 40 ml and a concentration of 10 mg/L of sodium chloride were prepared. The chemicals used in the research were from the German Merck Company in the laboratory type. Diluted HCl and NaOH were used to adjust pH. All experiments were carried out at a constant temperature and within the range of 20±2 °C.

2.1. Preparation and characterization of the sorbent

Rice husk was collected from rice milling factory and wheat straw was collected from agricultural farms. The prepared waste was first washed with distilled water, dried at 70 °C for 24 h, and then, mechanically crushed into a mixer. Finally, sieve No. 200 was used to prepare the nanometer sorbents. The morphological characteristics of sorbents were assessed using particle size analysis (Malvern), made in Germany Scanning Electron Microscopy (JSM-840A), made in Japan and the sorbent infrared spectrum was evaluated infrared spectrometer (Bruker ALPHA) manufactured by Bruker Optic in Germany. AZ 86505 pH meter was used to record the pH of the solutions and the 405 G flame photometer device made in Iran was applied to determine the final concentration of the soluble sodium.

The methylene blue adsorption method was used to measure the sorbent specific surface area. In order to determine the sorbent specific surface area, 1, 5, 10, 15, and 20 mg/L of Methylene blue were prepared to plot the calibration chart. Their concentration was measured and recorded by the flame photometer device. Then, 0.1g of sorbents was poured in 100 ml of 17.46 mg/L solution of methylene blue and placed on the shaker at 150rpm for one hour. The final concentration was measured after removing the sorbent from the solution with a filter paper (Whatman 42), and the sorbent- specific surface area was calculated by Equation 1 (Bestani et al., 2008).

$$S_g=b\frac{N_A}{M_{MB}}\sigma_{MB} \quad (1)$$

In which, b is the adsorption capacity obtained from the adsorption curve (mg/mg), N_A is the Avogadro number 6.02×10^{23}, M_{MB} is the molecular weight of methylene blue as much as 319.85 g/mol, σ_{MB} is the occupied space by adsorbed methylene blue as much as 1.08 nm^2, and S_g is the sorbent specific surface area based on the m^2/g.

In order to determine the density of the studied sorbents, a certain volume of each of the sorbents was initially weighted. Then, the samples were placed in an oven at 105 °C for 24 h to dry. The dried samples were weighed again. The weight difference of the samples before and after drying was equal to dry weight. Finally, the density of sorbents was determined using the following equation.

$$\rho=\frac{m_s}{v_t} \quad (2)$$

In which, m_s is the dry weight of the sample (g), v_t is the total sample volume (mm), and ρ is the density. The moisture weight of the sorbents was determined using the method described in ASTM (D2867-99). In order to determine the moisture weight of each sorbent, a certain mass of the sorbent was weighed and placed in an oven at 105 °C for 24 h to dry the sample. After the mentioned time and cooling, the sample and the container were weighed again. The following equation was used to determine the amount of moisture weight of the sorbent masses:

$$Moistureweight\%=\frac{(C-D)}{(C-B)}\times100 \quad (3)$$

In which, B is the sampling container; C is the weight of the container and the primary sample; and D is the weight of the container and the dried sample.

2.2. Adsorption experiments

2.2.1. Determine optimal pH

The purpose of this step of the experiment was to determine the optimal pH for the removal of sodium ions at a concentration of 10 mg/L. The solution pH is an important parameter in the process of adsorption (Zhao et al., 2015). Therefore, it is necessary to conduct experiments related to the effects of this parameter on the adsorption rate before any other test. In order to determine the optimum pH of adsorption, 1 g of the sorbents was poured into 36 falcons (for 3 replicates) and 40 ml of a metal solution was added at a concentration of 10 mg/L. The pH of the solutions was adjusted in the range of 3-8, then, they were placed on the shaker at a controlled temperature for 2 h and 120 rpm. Then, the samples were passed through carved filter paper and the concentration of the samples from the test was measured using a flame photometer (405 G, manufactured in Iran). In addition to the above, pH_{pzc} (point of zero charge) of samples was also determined. First, 40 ml of 0.1% normal sodium chloride solution was poured into several falcons. The pH of the samples was adjusted in the range of 10-2 using 0.1% normal hydrochloric acid (HCl) and 0.1% normal sodium hydroxide (NaOH). Then, 0.5

g of sorbent dosage was added to each falcon and the samples were placed on the shaker at 120 rpm for 24 h. After a period of time, the final pH of the samples was measured using a pH meter (Rivera et al., 2001; Órfão et al., 2006).

In this study, the removal efficiency percent and adsorption capacity of sodium ions were calculated by Equation 4 and 5, respectively:

$$\%R = \frac{C_i - C_f}{C_i} \times 100 \quad (4)$$

$$q = \frac{C_i - C_f}{m} \times V \quad (5)$$

In which, q is the adsorption rate of the dissolved material per unit mass of the sorbent (mg/g), C_i is the initial concentration of the soluble substance (mg/g), C_f is the concentration of the residual soluble substance (mg/g) after the equilibrium time, m is the sorbent (g) and V is the volume of the solution (L).

2.2.2. *Desorption experiments of sodium ions for the studied sorbents*

The desorption experiment was carried out after adsorption tests and isolation of sorbents from the solution. To this end, 40 ml of 0.1 normal hydrochloric acids was added to the optimal amount of sorbent and placed on the shaker at a speed of 120 rpm (Anirudhan et al., 2007; Mohammad et al., 2010; Singha and Das, 2013). After the time spent in the adsorption experiments (Chatterjee and Woo, 2009), the sample was centrifuged for 15 minutes at a rate of 2000 rpm to completely separate the solid phase (sorbent nanostructure particles). Then they were passed through craved filter paper and the concentration of desorbed samples was measured using the flame meter (model 405 G). The desorption process took place in five cycles (Anirudhan and Sreekumari, 2011). The percentage of metal ions removed from the sorbent was calculated using the following equation:

$$Desorption\ (\%) = \frac{\text{desorbed amount of solute}}{\text{absorbed amount of solute}} \times 100 \quad (6)$$

The numerator is the desorbed sodium ions (mg/L), and the denominator is the amount of absorbed sodium ions (mg/L).

2.2.3. *Absorption kinetics experiments*

To do the absorption kinetics experiment, 0.5 g of sorbent dosage was poured in a falcon containing 40 ml of a metal solution with 120 mg/L initial concentration and then, placed on the shaker at 120 rpm for duration of 10 to 180 minutes (Kumar and Bandyopadhyay, 2006). After mixing and isolation of solid phase from the liquid, the sodium concentration was measured by the 405 G flame meter made in Iran, and the kinetic models of Ho et al., Lagergren, intraparticle, power, and Elovich were used to describe the data (Hou et al., 2018).

2.2.4. *Absorption isothermic experiments*

To do the absorption isothermic experiment, 0.5 g of sorbent dosage was poured in a falcon containing 40 ml of a metal solution with 5 to 120 mg/L initial concentration and then, placed on the shaker at 120 rpm. After passing the equilibrium time, the samples were passed through the craved filter paper and the concentration of the samples from the experiment was measured using a flame meter (Model 405 G). Then, the Freundlich, Langmuir, Langmuir-Freundlich, Temkin, Halsey, and Dubinin-Radushkevich models were fitted on the data. The kinetic and isotherm models used in this study are presented in Table 1 and the introduction of the parameters of these models is given in Table 2.

Table 1. Equation of the models used in this research.

Model Name	Nonlinear Equation
Ho et al., (kinetics)	$q_t = \frac{K_2 q_e^{\,2} t}{1 + q_e k_2 t}$
Lagergren (kinetics)	$q_t = q_e(1 - \exp(-k_1 t))$
Intraparticle (kinetics)	$q_t = k_p t^{1/2} + I$
Power (kinetics)	$q_t = at^b$
Elovich (kinetics)	$qt = \left(\frac{1}{\beta}\right)\ln(\alpha\beta) + \left(\frac{1}{\beta}\right)\ln t + t0$
Freundlich (isotherm)	$q_e = kC_e^{1/n}$
Langmuir (isotherm)	$q_e = \frac{bq_m C_e}{(1 + bC_e)}$
Langmuir-Freundlich (isotherm)	$q_e = \frac{bq_m C_e^{\,1/n}}{(1 + bC_e^{\,1/n})}$
Temkin (isotherm)	$q_e = b_T.\mathrm{Lnk}_T + b_T.\mathrm{LnC}$
Halsey (isotherm)	$Lnq_e = \left[\left(\frac{1}{n_H}\right).Lnk_H\right] - \left(\frac{1}{n_H}\right).Ln\left(\frac{1}{Ce}\right)$
Dubinin-Radushkevich (isotherm)	$Lnq_e = Lnq_m + K\varepsilon^2$ $\varepsilon = RTLn(1 + {}^1/_{C_e})$

Table 2. Parameters of the models used in this research.

Coefficients	Definition
qt (mg/g)	absorbed ion dosage in time t
qe (mg/g)	absorbed ion dosage in equilibrium
k_1 (min)	Fixed adsorption
k_2 (g/mg/min)	Absorption rate
k_p (g/mg/$\frac{1}{2}$min)	Equation constant
I	Equation Intercept (dimensionless)
α (mg/g/min)	The initial absorption rate
β (g/mg)	Desorption constant
a, b	Equation constant (dimensionless)
C_e (mg/L)	The concentration of the absorbed substance in equilibrium in the liquid phase
b (L/mg)	energy absorption constant (L/mg)
q_m (mg/g)	Maximum Balancing Capacity to complete a layer
n	Sorbent Adsorption Capacity (Dimensionless)
k	Sorbent Adsorption Rate (Dimensionless)
b_T (J/mol)	The constant coefficient of adsorption heat
K_T (L/g)	Temkin experimental equilibrium coefficient
n_H	Power coefficient (Dimensionless)
K_H	Halsey constant coefficient (Dimensionless)

2.3. Models evaluation test

The use of efficient models for the goodness of fit of the data from adsorption experiments is one of the most important parts of studies on the adsorption and purification of wastewater. Hence, the use of evaluation methods for these models is very important. There are different RMSE, R^2, MBE, and Ferror to evaluate the models, which have been used in various resources (Gimbert et al., 2008).

To evaluate the models used in this research, RMSE (Root Mean Square Error), and R (Coefficient of determination) were used. The lower value of RMSE indicates that the fitted values are closer to the actual values, the R^2 value is close to one, represents the high correlation between the fitted values and the obtained values.

$$RMSE = \sqrt{\frac{\sum_{i=1}^{n}(q_e - q_c)^2}{n}} \tag{7}$$

$$R^2 = \left[\frac{\sum_{i-1}^{N}(qc-qcm)(qe-qem)}{\sqrt{\sum_{i-1}^{N}(qc-qcm)^2}\sqrt{\sum_{i-1}^{N}(qe-qem)^2}}\right]^2 \tag{8}$$

In which, q_C is the value obtained from the goodness of fit of the mode, q_e is the value obtained from the experiment; q_{cm} is the mean of the fitted model, q_{em} is the mean of the obtained result from the experiment, n is the number of components of the experiment.

3. Results and discussion

3.1. Characterization of sorbent

The results of the particle size analysis (PSA) of the Nanoparticle of the studied sorbent showed that 100% of wheat straw and rice husk wastes were in the range of nanostructures with a diameter of less than 110 and 11.68 nm, respectively Fig. 1. The specific surface area of sorbents was determined using the methylene blue adsorption method as much as 170.75 and 181.8 m^2/g. Table 3 shows the results of the characteristics of the studied sorbents. The SEM images shown in Fig. 2 show that the wheat straw and rice husk wastes have a complex, dense, rugged, and irregular structure, and deep ridges in the sorbents indicate an increase in the specific surface area and the heterogeneous energy distribution on the adsorbent. The results of ultraviolet fluorescence spectroscopy show the presence of potassium, calcium, silicon, copper, and zinc in the wheat straw and potassium, silicon, copper, and zinc in the rice husk wastes (Fig. 3). For both sorbents, the silicon element has the highest frequency. Since the studied sorbents do not have a gold element, the gold element in the analysis is related to the gold coating on the samples. FTIR was used to determine the functional groups in each sorbent.

Table 3. Physical properties of the studied sorbent.

Sorbent type (Nanostructure)	Specific surface area (m^2/g)	Solubility in water (Percentage)	Apparent specific weight (g/cm)	Moisture (Percentage)
Wheat Straw	170.75	11.33	0.12	4.768
Rice Husk	181.83	9.67	0.238	4.996

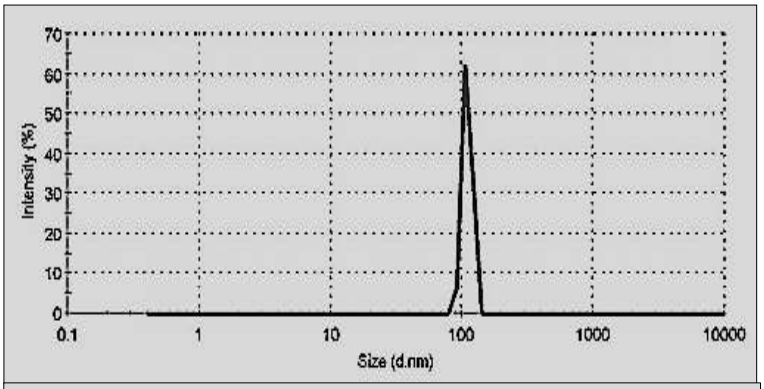

	Diam. (nm)	% Intensity	Width (nm)
Peak 1:	110.0	100.0	9.074
Peak 2:	0.000	0.0	0.000
Peak 3:	0.000	0.0	0.000

(A)

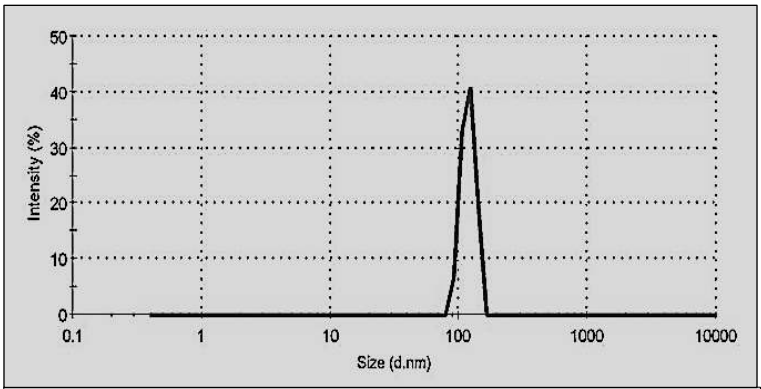

	Diam. (nm)	% Intensity	Width (nm)
Peak 1:	118.6	100.0	14.72
Peak 2:	0.000	0.0	0.000
Peak 3:	0.000	0.0	0.000

(B)

Fig. 1. Distribution of particle size of nanostructured sorbent, A**)** wheat straw, B**)** rice husk.

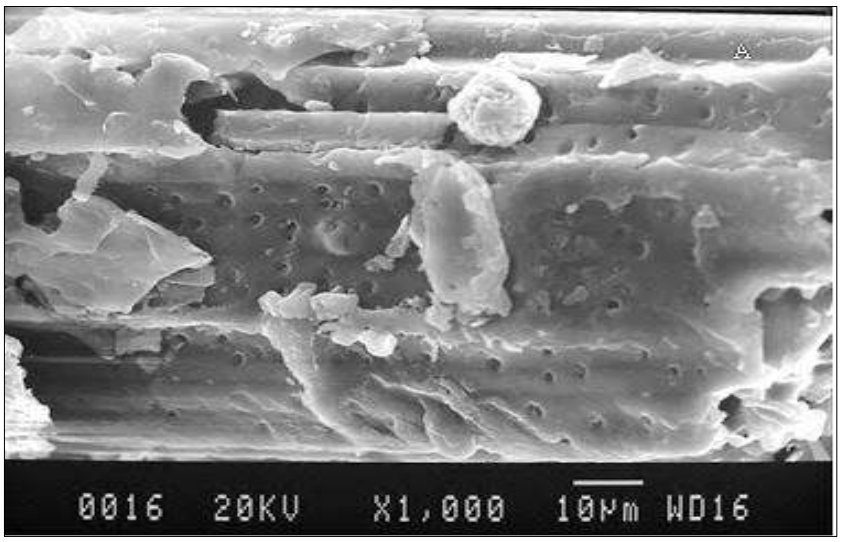

(A)

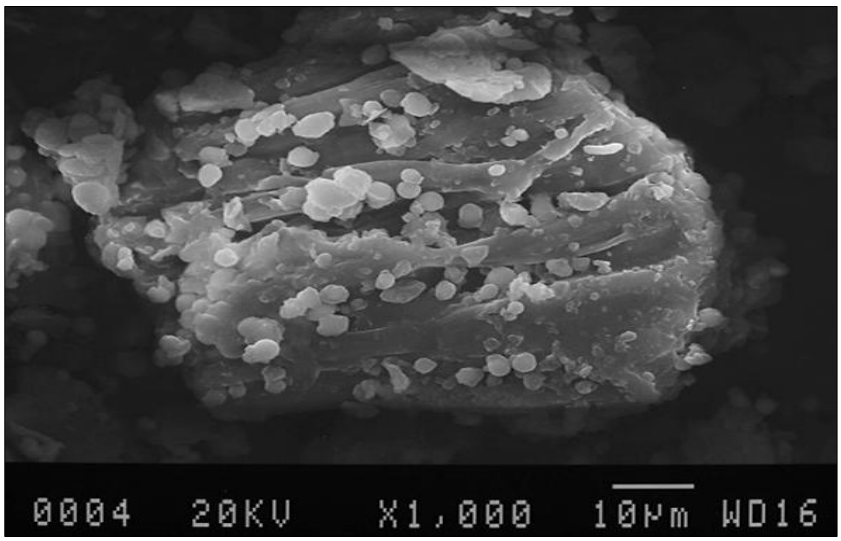

(B)

Fig. 2. The SEM image of powdered, A) wheat straw, B) rice husk.

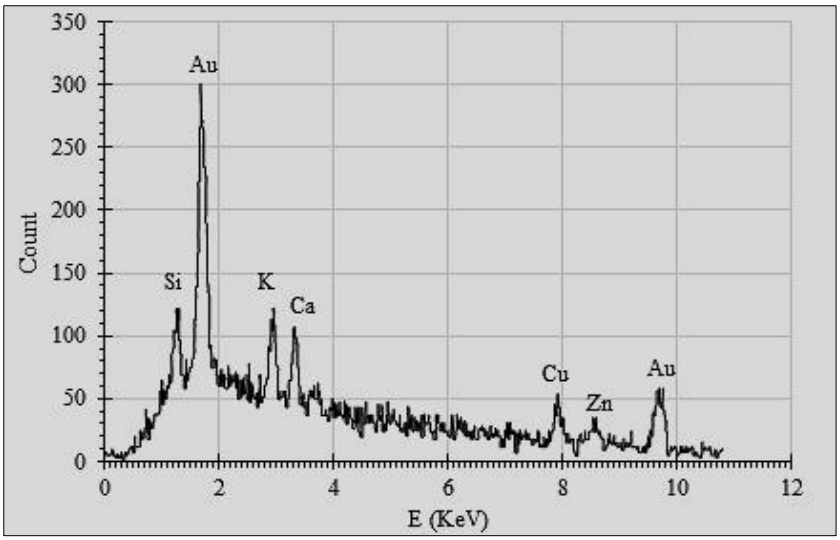

(A)

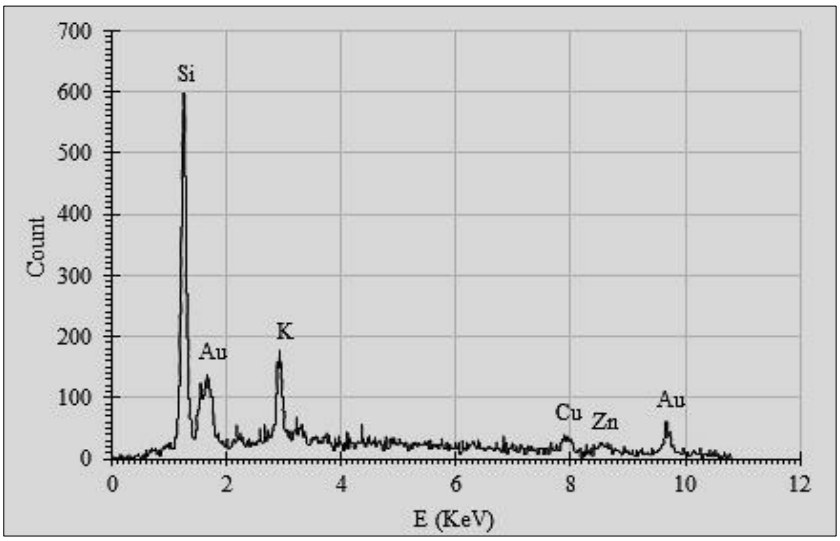

(B)

Fig. 3. X-ray diffraction pattern of powdered, A) wheat straw, B) rice husk.

Fig. 4 is related to the IR spectrum of the studied sorbents before adsorption. The linked vibrating frequencies for wheat straw are the wavelength peak as much as 3405.89 cm^2 corresponded to the symmetrical tensile vibrations of hydrogen OH...OH bonds, the wave frequency of 2921.41 cm^2 related to the tensile C-H bond, the wavelength of 1731.75-1628.99 cm^2 corresponds to the tensile C=O bond and the adsorption peak of 1053.53 cm^2 for the C-O bond. The frequencies for the rice husk are the wavelength of 3388.03 cm^2 related to the average absorption of symmetrical tensile vibrations of OH…OH bonds, the frequency peak of 2925.70 cm^2 related to the tensile vibrations of the C-H bond (alkaline group), the wavelength 1655.58/cm for tensile vibrations of the C=O bond (ester and amide group), and adsorption peak of 1055.93 cm^2 related to the C-O bond (esters group).

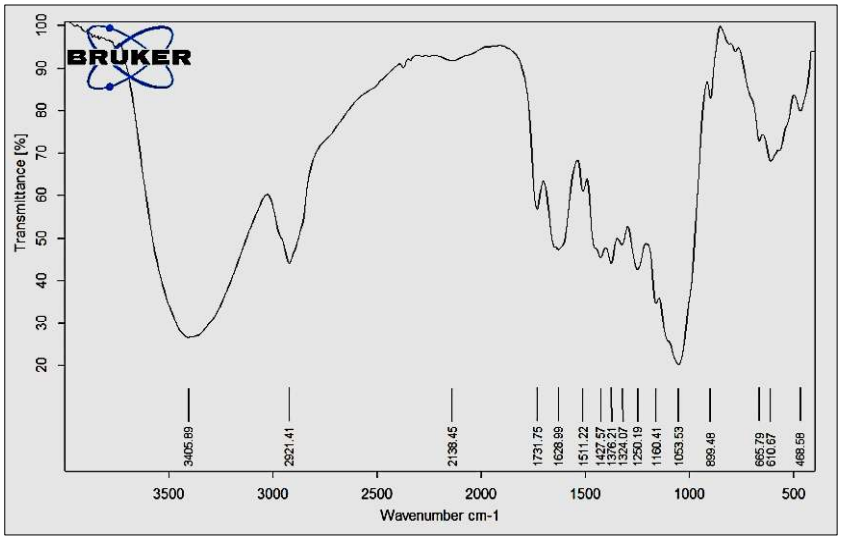

(A)

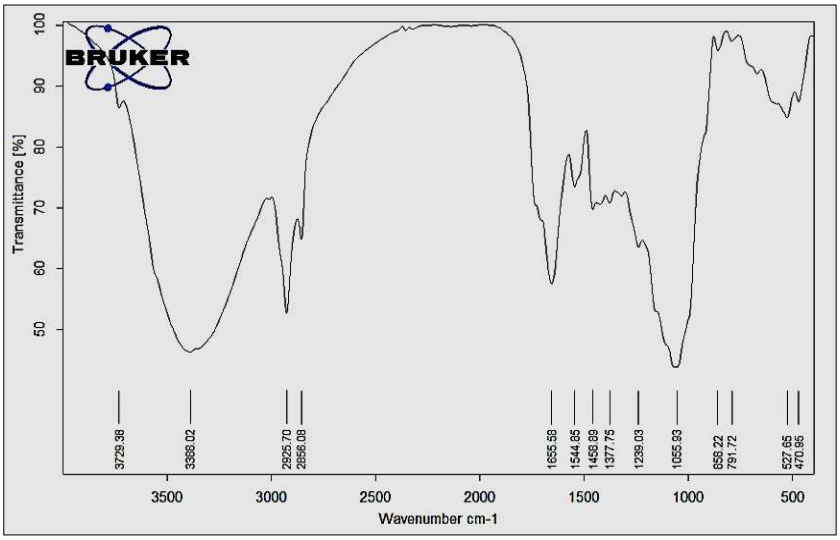

(B)

Fig. 4. FTIR spectrum of powdered, A**)** wheat straw, B**)** rice husk.

3.2. Effect of various parameters

3.2.1. Effect of pH

The results of the effect of the initial pH of the solution on the adsorption of sodium ions by the studied sorbents are shown in Fig. 5. According to Fig. 5, the sodium absorption efficiency by sorbents has shown a steady and gradual increase with increasing the pH. The minimum absorption efficiency for wheat straw and rice husks were 79.5 and 84.23%, respectively at pH=3. With increasing pH, the adsorption efficiency of sodium increased to its maximum value i.e. 88.89 and 91.70%, respectively at pH=5. Then, the absorption efficiency

remained almost constant at higher pHs. Therefore, pH=5 was chosen as the optimum pH for sodium removal by Nano-sorbent. There are several reasons for increasing the absorption of sodium ions by the studied Nano-sorbents with increasing pH. One of them is that the adsorbent includes a large number of powered sites. At low pHs, the sorbent has a positive charge, so the competition between H+ and metal ions increases for adsorption sites, but this competition is reduced with increasing pH because these powered surfaces have negative charges. Thus, positive metal ions are absorbed by electrostatic forces.

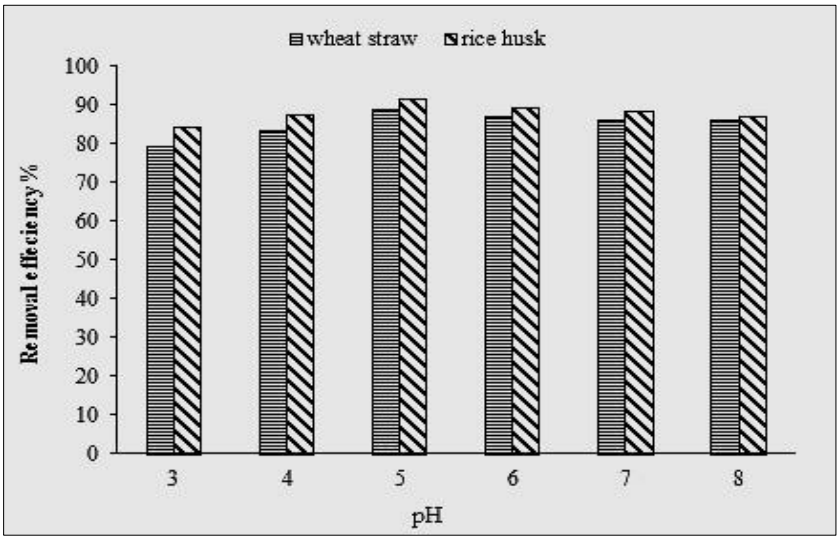

Fig. 5. Effect of pH on the removal of sodium by powdered adsorbents (sodium concentration: 10 mg/L, contact time: 120 min, sorbent dosage: 1 g and temperature: 20±2 °C).

3.2.2.1. The point zero charge determination

The pH_{pzc} of samples were also calculated in the range of pH=2-10, which are shown in Fig. 6. It is shown that the adsorbent has a combination of positive and neutral locations on the acidic side of pzc and a combination of negative and neutral locations on the alkaline side. Serencam et al., (2013) stated that if pH> pH_{pzc}, the sorbent level has a negative charge, pH<pHpzc, the sorbent level has a positive charge, and if pH=pH_{pzc}, the adsorbent is neutral (Serencam et al., 2013). The pH_{pzc} value for wheat straw and rice husk sorbents was 5.25 and 5.4, respectively. Since the optimum pH obtained from the test is less than the pH value was at the point of zero charge. Thus, the studied adsorbent has a positive charge. Consequently, the most adsorption of metal ions occurs on the adsorbents by non-electrostatic interactions such as chemical adsorption and deposition (Mahdavi et al., 2015).

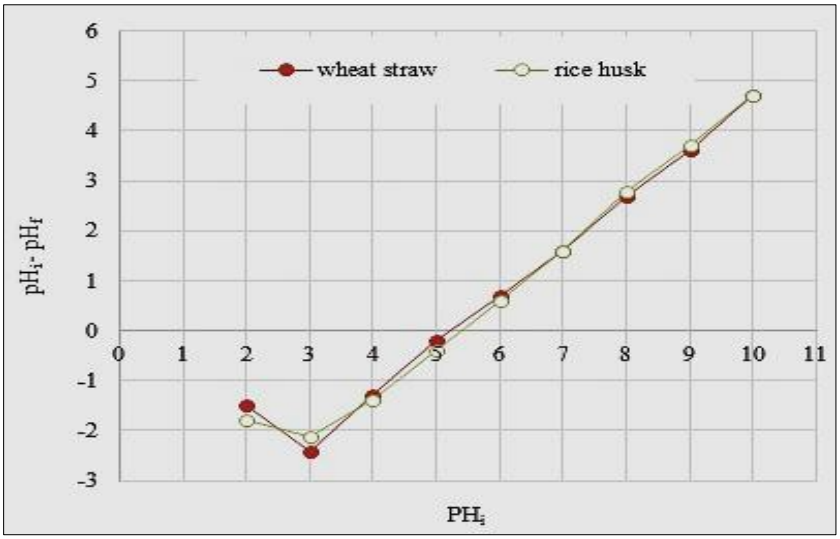

Fig. 6. pH_{pzc} point of zero charge for the studied sorbents.

3.2.3. Effect of adsorbent dosage

Fig. 7 shows the effect of sorbent on sodium adsorption by straw wheat and rice husk sorbents. As can be observed the sodium adsorption efficiency increased from 78.64 to 90.43% and 80.94 to 90.37% by increasing the sorbent dosage from 0.3 to 0.5 g, but no significant difference was observed in the absorption efficiency in more sorbent dosages because the specific surface area of nanoparticles is high. Therefore, they are highly reactive and react with each other by increasing the sorbent dosage in the solution instead of adsorbing the elements and come in the form of a hunch. Therefore, the absorption efficiency of sodium ion is constant by nanoparticles. Generally, the increase of removal efficiency enhances by increasing the sorbent mass due to the increase of the specific surface area and adsorption sites (Barka et al., 2008). Therefore, 0.5 g was chosen as the optimum mass for sodium removal.

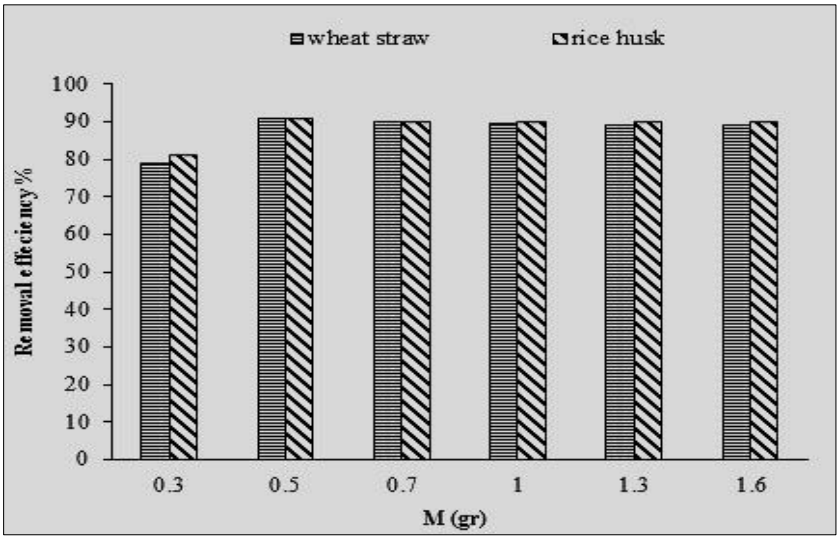

Fig. 7. Effect of sorbent mass on the removal of sodium by powdered adsorbents (sodium concentration: 10 mg/L, contact time: 30 min, pH: 5 and temperature: 20±2 °C).

3.2.4. Effect of contact time

The effect of equilibrium time on the sodium adsorption by the Nano-sorbents was investigated after determining the optimal pH. At this stage, 0.5 g of the sorbent dosage and pH=5 were considered as constant parameters and the contact time was changed from 10 to 180 min for various concentrations. Fig. 8 shows the variations of the efficiency and adsorption capacity of sodium ions at different times by Nano-sorbents. According to the figure, the sodium adsorption rate by the studied Nano-sorbents was very high for all concentrations at the initial times so that more than 55% sodium was removed from the solution for different concentrations in the first 10 min. The results showed that the efficiency and adsorption capacity increased over time, but the adsorption rate decreased. After 30 min of contact time, the efficiency and adsorption capacity reached their maximum at all concentrations and then, the adsorption rate remained almost constant. The cause of this phenomenon can be due to the completion of the adsorption capacity of the studied sorbent. With sorbent saturation, the sodium absorption rate from the solution decreased and the two solid and liquid phases reached almost an equilibrium state. The sodium adsorption to adsorbent rate and the ion return rate from the adsorbent to the solution are equal. Therefore, the adsorption equilibrium time for sodium removal by both Nano-sorbent was 30 min.

3.2.5. Effect of initial concentration

The effect of the initial concentration of sodium ions on the adsorption efficiency by the Nano-sorbents is shown in Fig. 8. According to the figure, the removal percentage had a descending trend and the adsorption capacity had an Ascending trend with an increase in the initial concentration of sodium from 5 to 120 mg/L at

different times. At the low initial concentrations of the solution, the surface and availability to adsorbed sites are high, and as a result, metal ions are easily absorbed. At the high initial concentrations, the available adsorption sites are more limited and this reduces the percentage of adsorption of metal ions (Kahrizi et al., 2016).

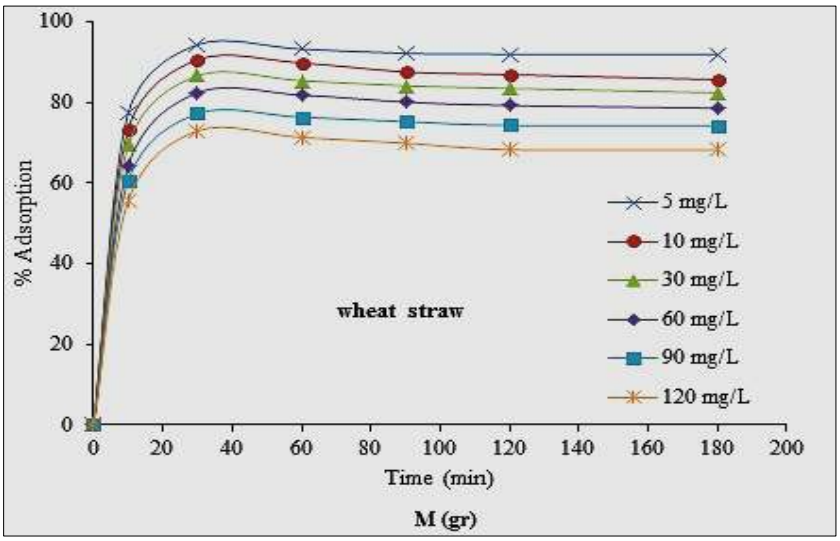

(A)

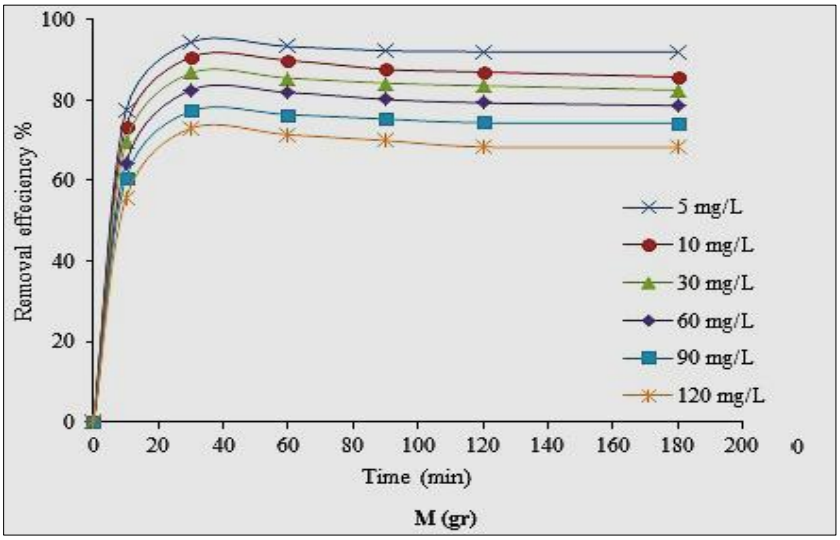

(B)

Fig. 8. Effect of contact time and initial concentration on Sodium removal (temperature, 20±2 °C, sorbent dosage, 0.5 g, and pH 5; A & B).

3.2.6. Investigation of adsorption-desorption reactions of the studied sorbents

The desorption percentage is to indicate the removal degree of the adsorbing substance from the sorbent. Regarding the optimal conditions obtained from adsorption experiments (sodium ions concentration, 10 mg/L, sorbent dosage, 0.5 g, contact time, 30 min, and pH=5), the desorption experiments were performed using 0.1% normal hydrochloric acid (Boparai et al., 2011; Zhang et al., 2010). The adsorption-desorption results of sodium ions using 0.1% normal hydrochloric acid are presented in five consecutive cycles in Fig. 9. According to the figure, the maximum adsorption efficiency of sodium ions for wheat straw and rice husk sorbents (89.89 and 92.19%, respectively) and the maximum desorption efficiency of sodium ions (37.16 and 39.63%, respectively) occurred in the first cycle and the 0.1% normal hydrochloric acid had a relatively low desorption capacity. The desorption efficiency decreased with increasing the desorption cycles so that the adsorption efficiency (52.38 and 59.12%, respectively) and the desorption efficiency (0.529 and 0.49%, respectively) of sodium ions for the studied sorbents reached the minimum at the fifth cycle. Comparing the sodium ion desorption percentage for

the studied sorbents in each of the five cycles showed that these sorbents are not recyclable and reusable and economically affordable.

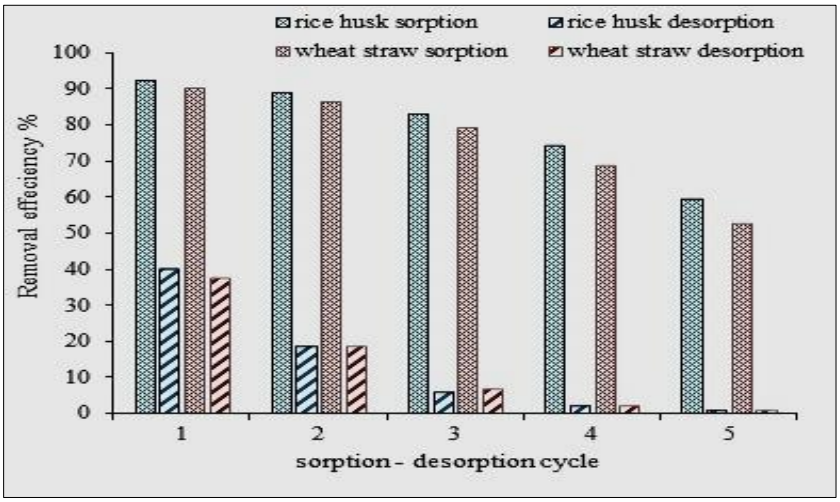

Fig. 9. The results of sodium ion desorption by the studied sorbents.

3.2.7. Adsorption kinetics

Important studies in the adsorption process are investigating the effect of contact time with the adsorption rate, which is known as kinetic studies. Fig. 8 shows the changes in the adsorption efficiency of sodium with time by the studied sorbents. As observed, the adsorption rate increases very much for both sorbents by increasing the contact time from zero to 30 minutes and then, decreased to a constant value after the desired time. Fig. 10 shows the goodness of fit of the kinetic models to the sodium adsorption laboratory data by the studied Nano-sorbents. Table 4 also shows the results of the goodness of fit of kinetic models. According to the table, the Lagergren model had the highest RMSE and Ho et al. model had the least RMSE among the studied models for both sorbents, and the highest R2 was more consistent with the adsorption data. The calculated adsorption capacity of sodium ion in the Lagergren model was less than the adsorption capacity of the data obtained from the experiment for the sorbent. The calculated adsorption capacity in Ho et al. model was more than the adsorption capacity of the data obtained from the experiment. Similar results were obtained for the adsorption of cadmium and cobalt by Diplotaxis and Chrysanthemums (Tounsadi et al., 2015); adsorption of copper, nickel, chromium, and zinc ions by a kind of *Moringa oleifera* (Drumstick tree) (Matouq et al., 2015); the adsorption of lead, copper, silver, and cadmium by polyacrylonitrile (Zhao et al., 2015); the adsorption of cadmium and mercury by modified nanoparticles of agricultural residues (Omorogie et al., 2014).

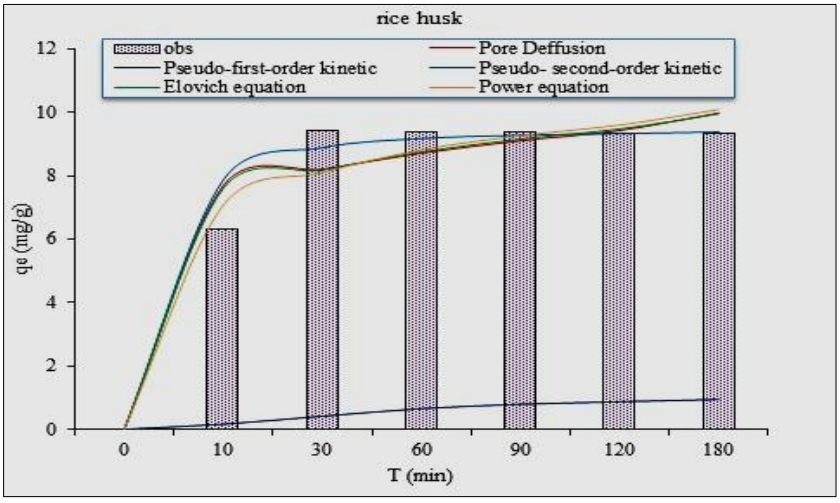

(A)

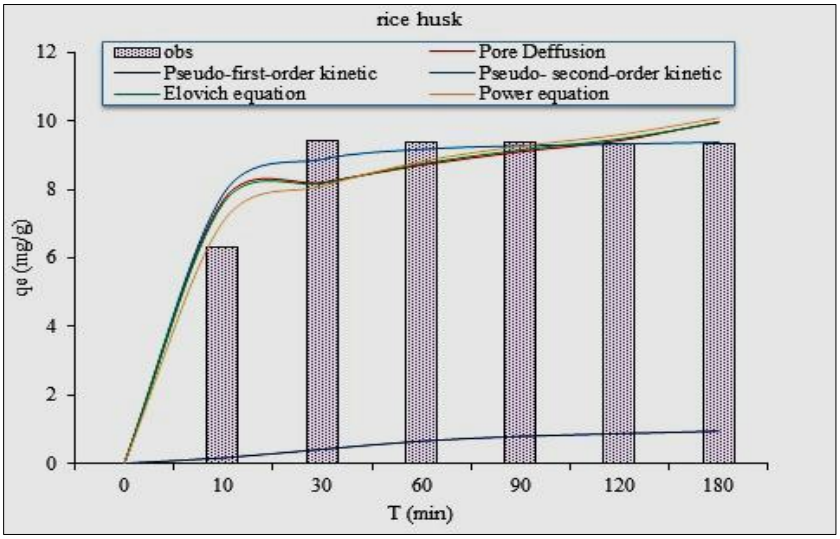

(B)

Fig. 10. The goodness of fit of the sodium adsorption kinetic models by the studied sorbents (A & B).

Table 4. Parameters of sodium adsorption kinetic models by rice husk sorbent.

Model Name	Parameter	Wheat straw	Rice husk
Pseudo-first-order kinetic	K^1	0.017	0.018
	qe (mg/g)	1.30	0.98
	R^2	0.55	0.58
	RMSE	8.15	8.27
Pseudo- second-order kinetic	K^2	0.08	0.05
	qe (mg/g)	9.43	9.49
	R^2	0.89	0.89
	RMSE	0.63	0.69
Power equation	A	5.96	5.33
	B	0.098	0.123
	R^2	0.59	0.59
	RMSE	0.63	0.75
Pore Diffusion	C	7.38	6.98
	k_P	0.19	0.22
	R^2	0.43	0.44
	RMSE	0.72	0.85
Elovich equation	A	24.83	7.56
	β	0.85	0.71
	R^2	0.47	0.48
	RMSE	0.70	0.83

3.2.8. Adsorption isotherms

Investigating the adsorption isotherm models shows the equilibrium correlation between the adsorbed substance in the adsorbent and the concentration of residual adsorption substance in the solution. Fig. 11 shows the isotherm models of sodium adsorption by the studied sorbents. In addition, the results of the goodness of fit of the models are given in Table 5. As can be observed, all models explain the data well except the two models of Temkin and Dubinin-Radushkevich at a confidence level of more than 95%. The RL index, which is used to assess the usability of the Langmuir Equation, is as follows.

$$R_L = \frac{1}{(1+bC_0)} \quad (9)$$

Table 5. Parameters of sodium adsorption isotherm models by the studied sorbents.

Model Name	Parameter	Wheat straw	Rice husk
Freundlich	K	0.11	0.113
	N	1.09	1.09
	R^2	0.99	0.99
	RMSE	0.23	0.31
Langmuir	b	0.002	0.002
	q_m	48.08	52.08
	R^2	0.97	0.97
	RMSE	0.31	0.36
Langmuir - Freundlich	b	0.002	0.002
	n	0.91	0.90
	R^2	0.97	0.97
	RMSE	0.47	0.38
Temkin	b_T	2.58	2.55
	K_T	0.16	0.17
	R^2	0.86	0.86
	RMSE	1.21	1.21
Halsey	n_H	1.09	1.09
	K_H	0.092	0.094
	R^2	0.97	0.97
	RMSE	0.28	0.36
Dubinin-Radushkevich	K	-10^{-5}	-10^{-5}
	q_m	4.80	4.97
	R^2	0.47	0.50
	RMSE	2.38	2.32

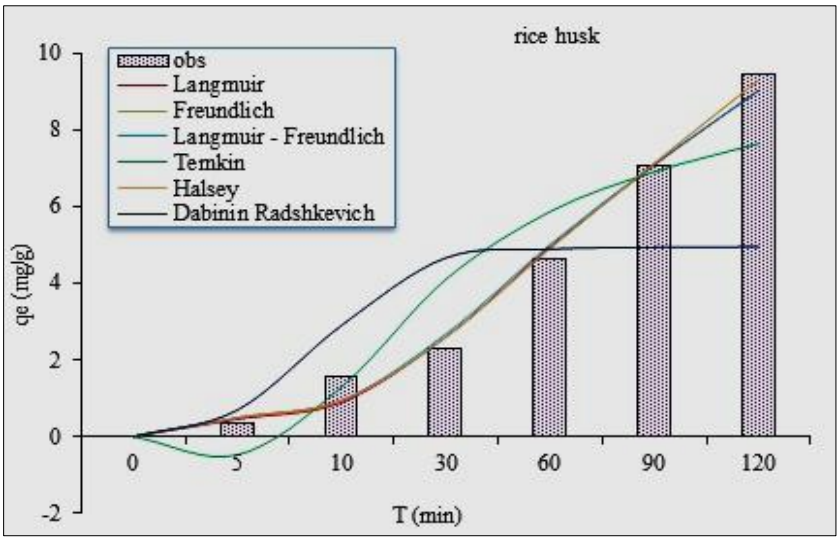

(A)

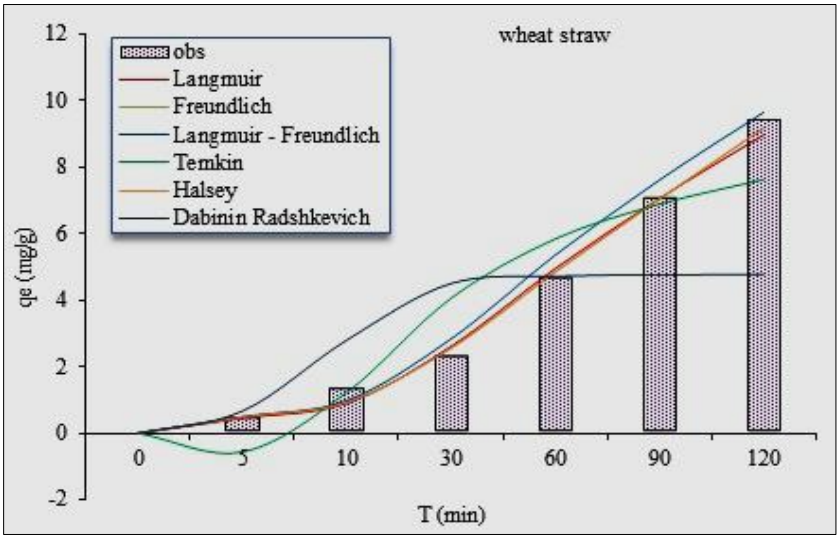

(B)

Fig. 11. The goodness of fit of the sodium adsorption isotherm models by the studied Nano-sorbents (A & B).

In which, C0 is the initial concentration of the solution and b is the Langmuir constant. If $R_L < 1$, then the model is inappropriate, if $R_L = 1$, then the linear state is appropriate if $0 < R_L < 1$, then the model is appropriate, and if $R_L = 0$, the model is inefficient. In this research, the R_L value for the wheat straw and rice husk was 0.81 and 0.83 (for the concentration of 120 mg/L), which shows that the Langmuir model has a good efficiency for the studied sorbents.

4. Conclusion

pH is one of the factors that greatly affect the adsorption efficiency, and the pH adjustment of the environments contaminated with metal cations is very important. Therefore, it is necessary to conduct the experiments related to the effect of this parameter on the adsorption rate before any other experiment (Afkhami et al., 2010). The results indicate that increasing the acidity of the dummy solution for both sorbents caused an ascending trend for the ion adsorption percentage, which reaches its maximum at pH=5. At pH higher than 5, sodium is deposited and the metal concentration reduction in the dummy solution is not due to its adsorption by the sorbent, but it is deposited due to increasing the pH of the environment and the increase in the concentration of hydrogen ions. Increasing the initial concentration of the solution from 5 to 120 mg/L resulted in a decrease in the adsorption of the metal in the solution by the studied sorbents, which can be attributed to the saturation of the sorbent particles. According to the results, the saturation capacity of wheat straw and rice husk sorbents in the concentration of 10 mg/L was 90.43 and 90.37 mg/g, indicating the high saturation capacity of the sorbents. The reaction rate was also very high, and 50% of the total amount of adsorption was done in the same minutes on average so that 55-77% of sodium was adsorbed after 10 min from the reaction at various concentrations. Of course, the initial adsorption depends on the type of sorbent. In the kinetic equations, the changes in concentration of the adsorbed substrate (qt) are shown with time.

According to Tables 4 and 5, Hou et al., model for the wheat straw and rice husk sorbents (RMSE=0.63, R^2=0.89) and (RMSE=0.69, R^2=0.89) and Freundlich isotherm for both sorbents with the highest R^2 (0.99) and the lowest RMSE (0.23 and 0.31, respectively) had better goodness of fit on the experimental data among the studied kinetic and isotherm models (Hou et al., 2018). The adsorption utility index (n in the Freundlich model) was as much as 1.09 for both sorbents, which indicates the desirability of adsorption because n should have values in the range of 1 to 10 to be considered as desirable adsorption. In the Elovich model, α represents the initial adsorption rate. The higher the amount of α, the greater the initial adsorption rate. $K_2q_e^2$ value in Ho et al. model represents the initial adsorption rate, and the adsorption of the pollutant by the sorbent is done more quickly in the higher rates. According to Table 3, the $K_2q_e^2$ value increased with the increasing initial

concentration of sodium ions (its maximum value for wheat straw and rice husk was as much as 7.11 and 4.59 min), which is probably because the thrust force has been increased for mass transfer by increasing the initial concentration of sodium ions.

The results of the goodness of fit of the kinetic models of Ho et al. and Lagergren on the experimental data showed that both nanostructured sorbents had a high adsorption capacity in removing sodium ions. The initial adsorption rate was determined using the Elovich and power model, which indicated the high initial adsorption rate of the sorbents. In addition, the effect of intraparticle diffusion in the initial stages of adsorption was investigated using the intraparticle diffusion equations. The results of the intraparticle diffusion model showed that this model did not determine the initial adsorption rate of sodium ions by the studied sorbents.

References

Afkhami, A., Saber-Tehrani, M., Bagheri, H., 2010. Simultaneous removal of heavy-metal ions in wastewater samples using nano-alumina modified with 2, 4-dinitrophenylhydrazine. *J. Hazard. Mater.*, **181**(1-3), 836-844. https://doi.org/10.1016/j.jhazmat.2010.05.089

Anirudhan, T.S., Sreekumari, S.S., 2011. Adsorptive removal of heavy metal ions from industrial effluents using activated carbon derived from waste coconut buttons. *J. Environ. Sci.*, **23**(12), 1989-1998. https://doi.org/10.1016/S1001-0742(10)60515-3

Anirudhan, T.S., Unnithan, M.R., 2007. Arsenic (V) removal from aqueous solutions using an anion exchanger derived from coconut coir pith and its recovery. *Chemosphere*, **66**(1), 60-66. https://doi.org/10.1016/j.chemosphere.2006.05.031

Armesto, L., Bahillo, A., Veijonen, K., Cabanillas, A., Otero, J., 2002. Combustion behaviour of rice husk in a bubbling fluidised bed. *Biomass Bioenerg.*, **23**(3), 171-179. https://doi.org/10.1016/S0961-9534(02)00046-6

Asrari, E., Tavallali, H., Hagshenas, M., 2010. Removal of Zn (II) and Pb (II) ions using rice husk in food industrial wastewater. *J. Appl. Sci. Environ. Manag.*, **14**(4), 159-162. https://doi.org/10.4314/jasem.v14i4.63306

Bakhshi, B., Rostami-Ahmadvandi, H., Fanaei, H., 2021. Camelina, an adaptable oilseed crop for the warm and dried regions of Iran. *Cent. Asian J. Plant Sci. Innov.*, **1**(1), 39-45. https://doi.org/10.22034/CAJPSI.2021.01.05

Barka, N., Qourzal, S., Assabbane, A., Nounah, A., Yhya, A.I., 2008. Adsorption of Disperse Blue SBL dye by synthesized poorly crystalline hydroxyapatite. *J. Environ. Sci.*, **20**(10), 1268-1272. https://doi.org/10.1016/S1001-0742(08)62220-2

Bestani, B., Benderdouche, N., Benstaali, B., Belhakem, M., Addou, A., 2008. Methylene blue and iodine adsorption onto an activated desert plant. *Bioresour. Technol.*, **99**(17), 8441-8444. https://doi.org/10.1016/j.biortech.2008.02.053

Boparai, H.K., Joseph, M., O'Carroll, D.M., 2011. Kinetics and thermodynamics of cadmium ion removal by adsorption onto nano zerovalent iron particles. *J. Hazard. Mater.*, **186**(1), 458-465. https://doi.org/10.1016/j.jhazmat.2010.11.029

Chaghakaboodi, Z., Kakaei, M., Zebarjadi, A., 2021. Study of relationship between some agro-physiological traits with drought tolerance in rapeseed (*Brassica napus* L.) genotypes. *Cent. Asian J. Plant Sci. Innov.*, **1**(1), 1-9. https://doi.org/10.22034/CAJPSI.2021.01.01

Chatterjee, S., Woo, S.H., 2009. The removal of nitrate from aqueous solutions by chitosan hydrogel beads. *J. Hazard. Mater.*, **164**(2-3), 1012-1018. https://doi.org/10.1016/j.jhazmat.2008.09.001

El-Sadaawy, M., Abdelwahab, O., 2014. Adsorptive removal of nickel from aqueous solutions by activated carbons from doum seed (Hyphaenethebaica) coat. *Alex. Eng. J.*, **53**(2), 399-408. https://doi.org/10.1016/j.aej.2014.03.014

Farokhian, S., Nejad, E.T., Nejad, G.M., 2021. Studying the Effect of Biofertilizers on the yield of *Sesamum indicum* Genotypes under Drought Stress. *Cent. Asian J. Plant Sci. Innov.*, **1**(1), 32-38. https://doi.org/10.22034/CAJPSI.2021.01.04

Gao, H., Liu, Y., Zeng, G., Xu, W., Li, T., Xia, W., 2008. Characterization of Cr (VI) removal from aqueous solutions by a surplus agricultural waste—rice straw. *J. Hazard. Mater.*, **150**(2), 446-452. https://doi.org/10.1016/j.jhazmat.2007.04.126

Gimbert, F., Morin-Crini, N., Renault, F., Badot, P.M., Crini, G., 2008. Adsorption isotherm models for dye removal by cationized starch-based material in a single component system: error analysis. *J. Hazard. Mater.*, **157**(1), 34-46. https://doi.org/10.1016/j.jhazmat.2007.12.072

Gupta, V.K., Jain, C.K., Ali, I., Sharma, M., Saini, V.K., 2003. Removal of cadmium and nickel from wastewater using bagasse fly ash—a sugar industry waste. *Water Res.*, **37**(16), 4038-4044. https://doi.org/10.1016/S0043-1354(03)00292-6

Haghshenas, H., Ghanbari Malidarreh, A., 2021. Response of yield and yield components of released rice cultivars from 1990-2010 to nitrogen rates. *Cent. Asian J. Plant Sci. Innov.*, **1**(1), 23-31. https://doi.org/10.22034/CAJPSI.2021.01.03

Han, R., Zhang, J., Zou, W., Xiao, H., Shi, J., Liu, H., 2006. Biosorption of copper (II) and lead (II) from aqueous solution by chaff in a fixed-bed column. *J. Hazard. Mater.*, **133**(1-3), 262-268. https://doi.org/10.1016/j.jhazmat.2005.10.019

Hou, Z., Chen, F., Wang, J., François-Xavier, C.P., Wintgens, T., 2018. Novel Pd/GdCrO3 composite for photo-catalytic reduction of nitrate to N2 with high selectivity and activity. *Appl. Catal. B- Environ.*, **232**, 124-134. https://doi.org/10.1016/j.apcatb.2018.03.055

Juang, R.S., Lin, S.H., Wang, T.Y., 2003. Removal of metal ions from the complexed solutions in fixed bed using a strong-acid ion exchange resin. *Chemosphere,* **53**(10), 1221-1228. https://doi.org/10.1016/S0045-6535(03)00578-2

Kahrizi, H., Bafkar, A., Farasati, M., 2016. Effect of nanotechnology on heavy metal removal from aqueous solution. *J. Cent. South Univ.,* **23**(10), 2526-2535. https://doi.org/10.1007/s11771-016-3313-8

Kingston, F.J., Posner, A.M., QUIRK, J.T., 1972. Anion adsorption by goethite and gibbsite: I. The role of the proton in determining adsorption envelopes. *J. Soil Sci.*, **23**(2), 177-192. https://doi.org/10.1111/j.1365-2389.1972.tb01652.x

Kumar, U., Bandyopadhyay, M., 2006. Sorption of cadmium from aqueous solution using pretreated rice husk. *Bioresour. Technol.*, **97**(1), 104-109. https://doi.org/10.1016/j.biortech.2005.02.027

Liang, H., Khan, Z.I., Ahmad, K., Nisar, A., Mahmood, Q., Ebadi, A.G., Toughani, M., 2020. Assessment of Zinc and Nickel Profile of Vegetables Grown in Soil Irrigated with Sewage Water. *Rev. Chim.*, **71**(4), 500-511. https://doi.org/10.37358/RC.20.4.8092

Mahdavi, S., Jalali, M., Afkhami, A., 2015. Heavy metals removal from aqueous solutions by Al 2 O 3 nanoparticles modified with natural and chemical modifiers. *Clean Technol. Environ. Policy,* **17**(1), 85-102. https://doi.org/10.1007/s10098-014-0764-1

Matouq, M., Jildeh, N., Qtaishat, M., Hindiyeh, M., Al Syouf, M.Q., 2015. The adsorption kinetics and modeling for heavy metals removal from wastewater by Moringa pods. *J. Environ. Chem. Eng.*, **3**(2), 775-784. https://doi.org/10.1016/j.jece.2015.03.027

Mohammad, M., Maitra, S., Ahmad, N., Bustam, A., Sen, T.K., Dutta, B.K., 2010. Metal ion removal from aqueous solution using physic seed hull. *J. Hazard. Mater.*, **179**(1-3), 363-372. https://doi.org/10.1016/j.jhazmat.2010.03.014

Montanher, S.F., Oliveira, E.A., Rollemberg, M.C., 2005. Removal of metal ions from aqueous solutions by sorption onto rice bran. *J. Hazard. Mater.*, **117**(2-3), 207-211. https://doi.org/10.1016/j.jhazmat.2004.09.015

Omorogie, M.O., Babalola, J.O., Unuabonah, E.I., Gong, J.R., 2014. Solid phase extraction of hazardous metals from aqua system by nanoparticle-modified agrowaste composite adsorbents. *J. Environ. Chem. Eng.*, **2**(1), 675-684. https://doi.org/10.1016/j.jece.2013.11.007

Órfão, J.J.M., Silva, A.I.M., Pereira, J.C.V., Barata, S.A., Fonseca, I.M., Faria, P.C.C., Pereira, M.F.R., 2006. Adsorption of a reactive dye on chemically modified activated carbons-influence of pH. *J. Colloid Interface Sci.*, **296**(2), 480-489. https://doi.org/10.1016/j.jcis.2005.09.063

Rivera-Utrilla, J., Bautista-Toledo, I., Ferro-García, M.A., Moreno-Castilla, C., 2001. Activated carbon surface modifications by adsorption of bacteria and their effect on aqueous lead adsorption. *J. Chem. Technol. Biotechnol.*, **76**(12), 1209-1215. https://doi.org/10.1002/jctb.506

Samadi, M.T., Saghi, M.H., Ghadiri, K., Hadi, M., Beikmohammadi, M., 2010. Performance of simple Nano Zeolite Y and modified Nano Zeolite Y in phosphor removal fromaqueous solutions. *Iran. J. Health Environ.*, **3**(1), 27-36.

Serencam, H., Ozdes, D., Duran, C., Tufekci, M., 2013. Biosorption properties of Morus alba L. for Cd (II) ions removal from aqueous solutions. *Environ. Monit. Assess.*, **185**(7), 6003-6011. https://doi.org/10.1007/s10661-012-3001-6

Sfaksi, Z., Azzouz, N., Abdelwahab, A., 2014. Removal of Cr (VI) from water by cork waste. Arab. J. Chem., **7**(1), 37-42. https://doi.org/10.1016/j.arabjc.2013.05.031

Singha, B., Das, S.K., 2013. Adsorptive removal of Cu (II) from aqueous solution and industrial effluent using natural/agricultural wastes. *Colloids Surf. Biointerfaces*, **107**, 97-106. https://doi.org/10.1016/j.colsurfb.2013.01.060

Tounsadi, H., Khalidi, A., Abdennouri, M., Barka, N., 2015. Biosorption potential of Diplotaxis harra and Glebionis coronaria L. biomasses for the removal of Cd (II) and Co (II) from aqueous solutions. *J. Environ.l Chem. Eng.*, **3**(2), 822-830. https://doi.org/10.1016/j.jece.2015.03.022

Xu, X., Gao, B.Y., Yue, Q.Y., Zhong, Q.Q., 2010. Preparation of agricultural by-product based anion exchanger and its utilization for nitrate and phosphate removal. *Bioresour. Technol.*, **101**(22), 8558-8564. https://doi.org/10.1016/j.biortech.2010.06.060

Zeidali, E., Korrani, H.M., Alizadeh, Y., Kamari, F., 2021. Ethnopharmacological survey of medicinal plants in semi-arid rangeland in western Iran. *Cent. Asian J. Plant Sci. Innov.*, **1**(1), 46-55. https://doi.org/10.22034/CAJPSI.2021.01.06

Zeidali, E., Roein, Z., Fathi, A., 2021. Study flora and distribution of weed (Case Study: fruit orchards of Darreh Shahr city, Ilam Province of Iran). *Cent. Asian J. Plant Sci. Innov.*, **1**(1), 10-22. https://doi.org/10.22034/CAJPSI.2021.01.02

Zhang, Z., Li, M., Chen, W., Zhu, S., Liu, N., Zhu, L., 2010. Immobilization of lead and cadmium from aqueous solution and contaminated sediment using nano-hydroxyapatite. *Environ. Pollut.*, **158**(2), 514-519. https://doi.org/10.1016/j.envpol.2009.08.024

Zhao, R., Li, X., Sun, B., Shen, M., Tan, X., Ding, Y., Jiang, Z., Wang, C., 2015. Preparation of phosphorylated polyacrylonitrile-based nanofiber mat and its application for heavy metal ion removal. *Chem. Eng. J.*, **268**, 290-299. https://doi.org/10.1016/j.cej.2015.01.061

Zulkali, M.M.D., Ahmad, A.L., Norulakmal, N.H., 2006. Oryza sativa L. husk as heavy metal adsorbent: optimization with lead as model solution. *Bioresour. Technol.*, **97**(1), 21-25. https://doi.org/10.1016/j.biortech.2005.02.007

How to cite this paper:
Rasouli, A., Bafkar, A., Chaghakaboodi, Z., 2020. Kinetic and equilibrium studies of adsorptive removal of sodium-ion onto wheat straw and rice husk wastes. *Cent. Asian J. Environ. Sci. Technol. Innov.*, **1**(6), 310-329.